Transparent and Mechanically Resistant Silver Nanowire based Low-Emissivity Coatings

Sébastien Hanauer[1], Caroline Celle[1], Chiara Crivello[2], Helga Szambolics[1], David Muñoz-Rojas[2], Daniel Bellet[2], Jean-Pierre Simonato[1]**

[1] Univ. Grenoble Alpes, CEA, LITEN, F-38054 Grenoble, France.

[2] Univ. Grenoble Alpes, CNRS, Grenoble INP, LMGP, F- 38000 Grenoble, France

KEYWORDS: metallic nanowires, energy saving window, encapsulation, protective layer, SALD

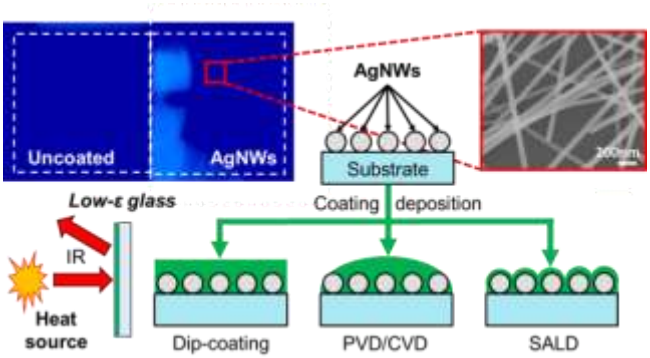

ABSTRACT

This article reports on the fabrication and investigation of low-emissivity (low-E) coatings based on random networks of silver nanowires (AgNWs). The transparent layers based on AgNWs do exhibit low emissivity while being still transparent: an overall emissivity as low as 0.21 at 78% total transmittance was obtained. A simple physical model allows to rationalize the emissivity-transparency dependence and a good agreement with experimental data is observed. This model demonstrates the role played by AgNWs which partially reflect IR photons emitted by the substrate, exacerbating then the presence of AgNWs and lowering the total emissivity. The potential use of such layers in functional devices is hampered by the poor intrinsic surface adhesion of the AgNWs, which renders the coating fragile and prone to mechanical damaging. Two very efficient encapsulation processes based on the deposition of a conformal alumina thin film using the Spatial Atomic Layer Deposition technique and the solution processed layer deposition of a polysiloxane varnish have been developed to thwart this weakness. Both coatings combine sturdy mechanical resistance relying on a strong interfacial adhesion and excellent optical transmittance properties. The performances for the mechanically resistant low-E coatings achieve an overall emissivity as low as 0.34 at 74% total transparency. The set of optical properties and mechanical resistance of the reported AgNWs based low-E coatings combined with the ease of fabrication and the cost-effective production process make it an excellent candidate for a wide set of applications, including smart windows for energy-saving buildings.

1. INTRODUCTION

The recent development of nanomaterials has generated hope in many fields. Interestingly some nanomaterials were initially developed for specific applications, but have opened new possibilities for other fields. Metallic nanowires, and in particular silver nanowires (AgNWs), raised at first great expectations for the fabrication of flexible transparent electrodes. Along carbon-based nanospecies,[1,2] metal meshes,[3] polymers[4–6] and many hybrid materials, AgNWs appear as a promising alternative to existing transparent conductive materials based on thin layers of oxides or metallic coatings.[7–10] Then other applications of interest such as sensors,[11,12] biomedical devices,[13] transparent film heaters,[14,15]and energy storage systems[16,17] to name but a few, based on the same building blocks have shown great potential. A still moderately reported application is related to their potential use as an efficient low-emissivity (low-E) layer. It relies on the low emissivity values in the mid-infrared range of AgNW based layers, while keeping high transparency in the visible range. Low-E transparent materials are of interest for several applications, like energy saving windows,[18] thermal camouflage,[19] or textiles for personal thermal management.[20]

Only very few reports have been published so far on the potential of AgNWs coatings for modulating IR emission. Larciprete *et al.* first reported that such coatings, *i.e.* random networks of AgNWs, could be valuable for IR signature reduction.[21] Bobinger *et al.* compared these coatings to uncoated glass, and pointed out that at high transparency (> 81%), the emissivity can be decreased by more than a factor of 2. This evidenced that AgNW thin films can efficiently block mid-infrared radiation, while keeping a high transparency in the visible and the near infra-red spectra.[22,23] Similar results were reported by Gupta *et al.*[24] and more recently a spray-coated

process based on AgNWs and polyvinylbutyral was reported.[25] Although preliminary, these results are promising when compared to the state of the art and further developments of this nanotechnology appear timely.[18]

In this article, emissivity and transmittance of AgNW networks associated to different densities are investigated. A simple physical model is proposed to understand the experimental relationship between emissivity and transmittance, a fairly good agreement is obtained between experimental data and the model. We also propose a straightforward process to fabricate low-E coatings based on encapsulated AgNWs. Due to their low intrinsic resilience to mechanical constraints like rubbing, peeling or scrapping, pristine AgNW networks must be physically protected by efficient coatings. However these encapsulating layers should not deteriorate the low-E performances of the active material. Several coatings deposited by dip-coating, vacuum processes and atmospheric pressure spatial atomic layer deposition (SALD) have been evaluated and compared through optical and mechanical characterizations.[26] Thin alumina coatings deposited by SALD lead to preserved low-E properties coupled with excellent mechanical resistance performances.

2. EXPERIMENTAL

2.1. Materials

All the chemical reagents received from Aldrich used in our experiments were analytical grade and were used as received without any further purification. Eagle XG^{TM} glass substrates made of alkaline earth boro-aluminosilicate type and 1.1 mm thick were purchased from Corning.

The production of AgNWs was realized according to a published protocol.[27] In a typical synthesis, silver nitrate $AgNO_3$ (0.68 g) was dissolved in 40 mL of ethylene glycol (EG) under slow stirring rate in a round flask. In another flask, polyvinylpyrrolidone (average mol. wt 40,000, 1.77g) and

NaCl (1 mM) were dissolved in EG (80 mL) at 120 °C. The solution was cooled to room temperature and then slowly added to the first flask within 9 min. The mixture was finally heated at 160 °C and cooled to room temperature. The purification of the AgNWs was realized by decantation.[28] At the end of the synthesis, the solution contains many nanoparticles (nanowires and metallic by-products) as well as remaining organics. One of the main issues after synthesis of nanowires is their separation from the reaction medium. Decantation leads to a straightforward purification of the solution. When the solution is at room temperature it is poured in a lipless beaker, covered with a watch-glass, and settled for two days. The settlement is noticeable after few hours, however the best results were obtained after two days. The remaining grey residue containing AgNWs is then diluted with MeOH to ensure good dispersion. The targeted concentration is typically in the order of 0.1 – 1.0 $g.L^{-1}$. The silver concentration was measured using an atomic absorption spectrometer (Perkin Elmer AAnalyst 400). The obtained solution is stable at least for months. The morphology analysis of AgNWs was performed on a ZEISS LEO 1530 FEG-SEM. Counting of the diameter and length dimensions was performed with the ImageJ software.

2.2. Deposition of AgNWs

Square 25x25 mm^2 glass substrates from Corning were used as substrate. Before deposition, the substrates were cleaned by sonication in an acetone/ethanol isovolumetric mix for 5 min, and then dried under air. To enhance the hydrophilicity of the samples and facilitate a homogeneous deposition of the AgNWs suspension, the substrates were treated by an oxygen plasma for 90 s. The deposition was carried out using a Sono-Tek ExactaCoat coating system. The substrates were placed on a heating plate at 130 °C. At thermal equilibrium, a 0.2 $mg.mL^{-1}$ (measured by atomic

absorption spectrometry on a Perkin Elmer AAnalyst 400) suspension of AgNWs in MeOH was spray-coated through a moving ultrasonic nozzle on the substrate.

2.3. Encapsulation

Networks of AgNWs deposited on glass substrates were encapsulated using different coating materials. Both spin-on glass (SOG) silica and a commercially available polysiloxane-based varnish from Isochem (AE12) were deposited by a dip coating method. For silica, the samples were dipped in the solution for 10 s, then extracted at a speed of 1 mm/s. For the encapsulation using AE12 varnish, the samples were dipped for 5 s and extracted at 0.75 $mm.s^{-1}$. The coating was then removed from the rear face of the substrates using ethanol, and the samples were annealed in an oven at 100 ºC for 1 h. Aluminum-doped zinc oxide (AZO) at 4% atomic doping was deposited using physical vapor deposition (PVD) MRC-603 system under 4 mTorr pressure at 2.4 $W.cm^{-2}$ RF power. Indium-tin-zinc-oxide (ITZO) layers were obtained by a PVD Alliance Concept DP1100 equipment with a In_2O_3-90%:SnO_2-3%:ZnO-7% target under $1.2x10^{-3}$ mbar at 0.7 $W.cm^{-2}$. The coatings of silicon oxycarbide (SiOC) layers were obtained by a plasma-enhanced chemical vapor deposition (PE-CVD) under 0.25 mbar at 0.22 $W.cm^{-2}$, from an octamethylcyclotetrasiloxane (OMCTSO) liquid precursor. AZO, zinc oxide (ZnO) and alumina (Al_2O_3) layers were deposited by a home-built SALD system[29,30]. Diethylzinc (STREM chemical) and Trimethylaluminum (GmbH) were used as the precursors, the speed motion was set to 200 $mm{\cdot}s^{-1}$ (170 $mm{\cdot}s^{-1}$ for Al_2O_3) with a distance between the head and the substrate of 150 µm.

2.4. Optical characterization

The total transmittance spectra between 380 nm and 780 nm were recorded using a UV-visible spectrometer Varian Cary 5000 equipped with an integrating sphere. Infrared total reflectance

spectra between 2 µm and 20 µm were recorded using a Bruker Equinox 55 FT-IR spectrometer equipped with an integrating sphere. The emissivity ε was then calculated according to equation (1):

$$\varepsilon\,(T,\lambda_1,\lambda_2) = \frac{\int_{\lambda_1}^{\lambda_2} L_\lambda^B(T)*(1-R_\lambda)\,d\lambda}{\int_{\lambda_1}^{\lambda_2} L_\lambda^B(T)\,d\lambda} \qquad \text{eq.(1)}$$

Where $\lambda_1 = 2$ µm and $\lambda_2 = 20$ µm, R_λ is the total reflectance of the sample at a wavelength λ and $L_\lambda^B(T)$ is the blackbody radiance at a temperature T, according to Planck's law:

$$L_\lambda^B(T,\lambda) = \frac{2hc^2}{\lambda^5\left(\exp\left(\frac{hc}{\lambda kT}\right)-1\right)} \qquad \text{eq.(2)}$$

where h, c and k are, respectively, Planck's constant, light celerity in vacuum and Boltzmann constant.

All calculations have been referenced to a blackbody at a temperature of 20 °C, as the range of temperature for low emissivity coating application varies from -50 °C to 100 °C.

2.5. Electrical characterization

The electrical resistance of thin films was determined using a 4-point probe method with a Loresta resistivity meter EP MCP-T360. For each sample, 5 measurements were conducted to calculate the average sheet resistance of the layer.

2.6. Mechanical characterization

To characterize the efficiency of the studied protective layers, two mechanical tests were used. Peel tests were performed using a 3M Scotch® Crystal tape. The tape was placed on top of the protective layer, on one half of the specimen area for the sake of comparison, and then removed.

It was thus possible to notice the potential degradation of the AgNW network with the naked eye. Cross-cut adhesion tests were also conducted on the samples according to the ISO 2409 Standard method. A 6-blades cutter was used to carve a lattice pattern through the coating. Tape was applied on the carved area of the sample and then quickly removed. Microscope images of the as-prepared samples were analyzed to determine the resistance of the protective layer. The capping layer was considered adhesive if less than 5% of the test area was degraded.

3. RESULTS AND DISCUSSION

The principle of low-emissivity coatings relies on the ability of the coating to reflect IR radiations in a certain wavelength range, and thus to help towards heat management. Typically, for energy saving windows, low-E coating reflects the heat back to the sun in the summer, while during winter the heat from the inside comes up against the Low-E coating, being reflected back into the house. This is schematized in Figure 1a-b and exemplified in Figure 1e-f-g and 1h-i. In the first example, two identical samples were prepared by spray-coating of AgNWs (Fig. 1 c-d), and placed behind substrates with and without AgNWs based low-E coating, and submitted to a calibrated IR radiation beam (see Figure 1e). Both vials contain the same thermochromic ink, which undergoes a color change at a specific temperature (blue ↔ white at 43±2 °C in this study). It can be observed that without low-E coating the temperature on the other side of the raw sample is higher, leading to a white color switch of the thermochromic ink (Figure 1f,g). Similarly, in Figure 1h, the two glass substrates with and without low-E coating were placed in front of an IR camera, at a distance of 50 cm. The substrate on the right was half-coated with an AgNWs layer. An experimenter

wearing glasses stood behind the IR camera, in a way that the IR radiations emitted by his face could be reflected by the substrates and detected by the IR camera (wavelengths 7.5 – 14.0 µm, see Figure 1i).

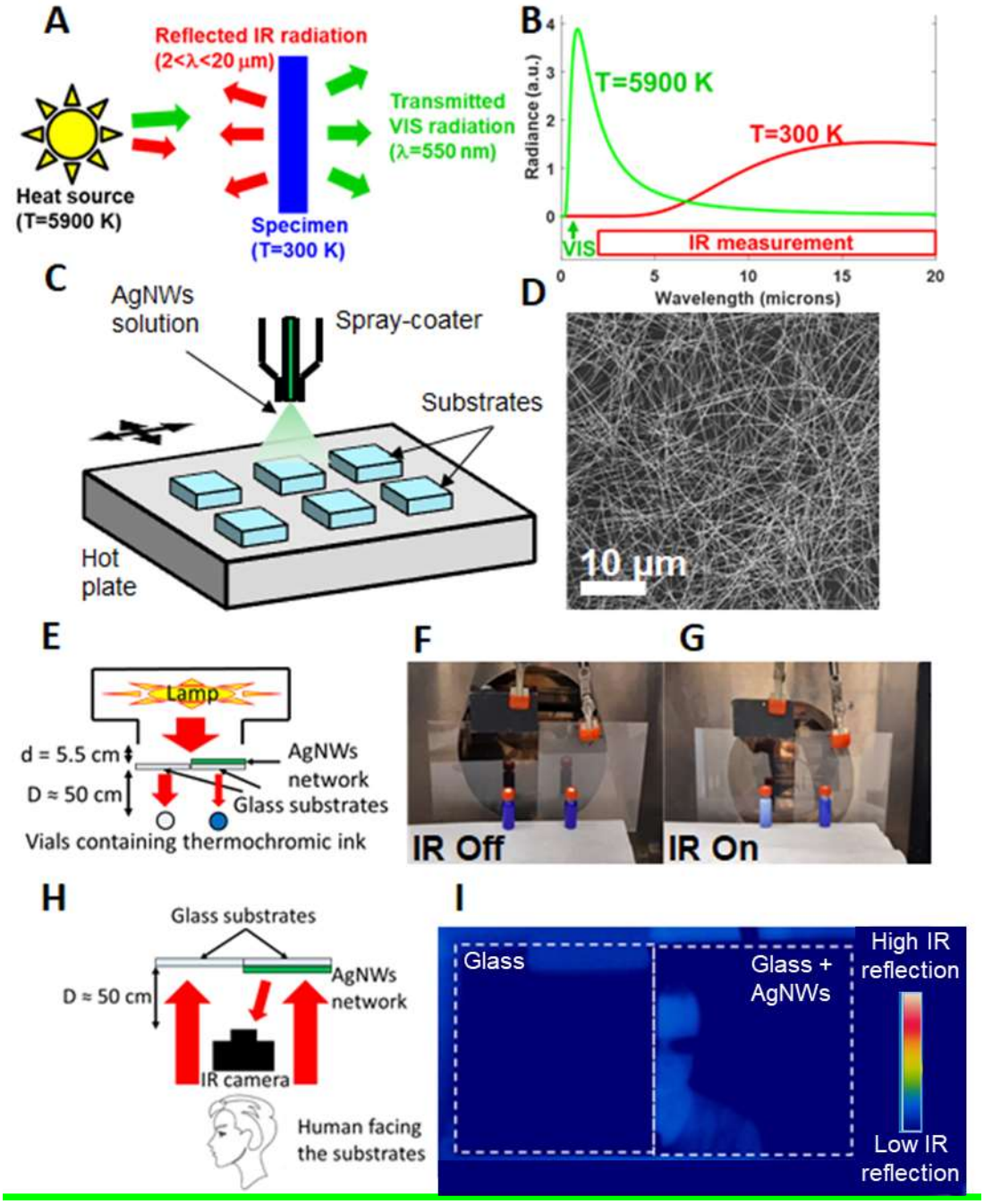

Figure 1. (a) Schematized principle of optical measurements: the specimen's transmittance is measured at the wavelength of 550 nm while the reflectance is measured over the range 2-20 µm. Low-E coatings can be useful during summer when IR light from the sun is mainly reflected while the transmittance in the visible is high; (b) black body radiance calculated at the heat source temperature (5900K), associated to the sun surface temperature, and a specimen at room temperature (300K). The latter has been multiplied by a factor 3,000 for the sake of comparison; (c) Scheme of the spray-coating process; (d) SEM image of a sprayed random network of AgNWs; (e) Schematic top view of the setup used to show IR reflective effect of two transparent 10x10 cm^2 samples (without and with AgNW coating on the left and on the right side respectively) on thermochromic ink samples (blue to white switching temperature at 43°C) and images of the actual setup and inks. The source was composed of three halogen lamps Haloline 750 W 230V R7S from OSRAM. (f) before and (g) after IR radiation; (h) Schematic top view of the setup used to show the IR reflective effect on the face of an experimenter and (i) associated IR images.

The low-E coatings were fabricated using AgNWs with dimensions of about 65 ± 12 nm in diameter and 6 ± 2 µm long. Samples with various coverage loadings (*i.e.* network density) were prepared in order to reach different transmittance values, the latter being correlated linearly with the areal mass density.[31,32] The emissivity values in the mid-IR range (2-20 µm) as a function of the transmittance (measured at $\lambda = 550$ nm) were plotted in Figure 2a and compared to other recent studies.[22,24,25] For low-E coatings, the searched area is situated at the bottom right of the figure, associated with low emissivity and large transmittance values.

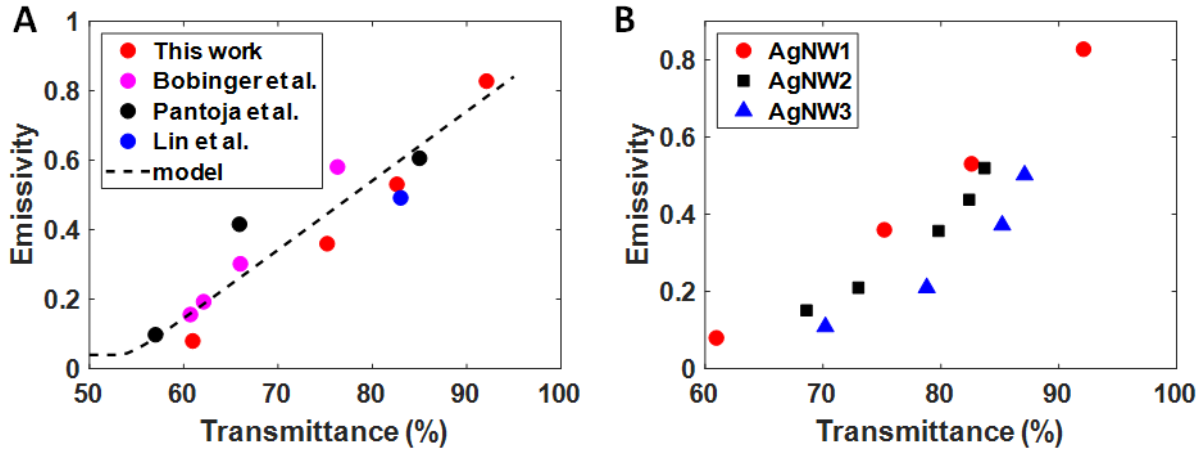

Figure 2. (a) Emissivity of AgNWs layers as a function of their total transmittance (measured at 550 nm, or 633nm for Pantoja et al.) and comparison with the state-of-the-art literature from Bobinger[22], Pantoja[24] and Lin[25] reports. Standard AgNWs (L= 6 µm and D= 65 nm) were used. The dashed line is associated to the model proposed in this article (see eq.(3)); (b) Impact of the AgNWs dimensions on the relation between emissivity and total transmittance (at 550 nm) of AgNW networks. The dimension of the nanowires are the following: AgNW1: L=6 µm and D=65 nm (FF=92, red dots), AgNW2: L=9 µm and D=93 nm (FF=97, black squares), AgNW3: L=15 µm and D=37 nm (FF=398, blue triangles).

The comparison indicates a similar trend, confirming that AgNWs films can exhibit a low emissivity at a high transparency, which renders this technology particularly relevant. For instance an emissivity value of 0.53 was measured at 82% transparency.

In order to rationalize the dependency between emissivity and transparency, a simple physical model is proposed here and developed further in the supplementary information. The relationship between the emissivity of the AgNW network, E_m, and its transparency, T_r, can be derived as follows:

$$E_m = \sqrt{{E_m^{Ag}}^2 + (E_m^{Ag} + E_m^{sub}(1-\eta) + (\eta.E_m^{sub} - E_m^{Ag}).T_r)^2} \qquad \text{eq.(3)}$$

where E_m^{Ag} and E_m^{sub} are the emissivity value of a very dense AgNW network (or silver) and bare glass substrate, respectively. E_m^{sub} was experimentally determined on the substrate, a value of 0.94 was measured.

As described in the SI, the coefficient η is associated to the fact that AgNWs do partially reflect IR photons emitted by the substrate, exacerbating the role played by the presence of AgNWs. This is for instance why, as shown in Figure 2a and 2b, for a transmittance below 60% (for which the areal surface fraction of the substrate covered by AgNWs is about 40%) the emissivity is already close to the one of silver. By construction the coefficient η is larger than unity, and is the only fitting parameter of this simple physical model. In other words if the AgNWs were to be replaced by perfectly flat Ag and substrate surfaces the coefficient η would be unity, though when considering its third dimension η is larger than unity. By considering that E_m^{Ag}, E_m^{sub} and η are respectively equal to 0.04, 0.94 and 2.17; a good agreement between the proposed model and the experimental data is observed, as shown in Figure 2a. In particular a linear relationship between the emissivity and the transparency is observed from 60 to 90% transparency, a range where most applications are considered.

This model sheds light on the key role played by the reflectance of AgNWs of IR photons emitted by the bare substrate. Therefore one can expect that the nanowires dimensions should play a role. Since the dimensions of the AgNWs can be controlled by adjusting the synthetic protocols,[27] three batches of different AgNWs were prepared to evaluate this potential. The average diameter (*D*) and length (*L*), as well as form factor (*FF*) which is the ratio of the length divided by the diameter are the following: AgNW1 (*D*=65 nm, *L*=6 μm, *FF*=92); AgNW2 (*D*=93 nm, *L*=9 μm, *FF*=97) and AgNW3 (*D*=37 nm, *L*=15 μm, *FF*=398). The influence of AgNWs dimensions on the

emissivity-transmittance dependence is observed in Figure 2b. The same tendency observed in Figure 2a is reported but with slightly different η values. The fine dependence of η upon AgNWs dimensions on the emissivity-transparency relationship appears complex, it is considered beyond the scope of this article. However one can already observe that thinner and longer AgNWs (associated to large *FF* values) can be of interest for low-E coatings since the network fabricated with AgNW3 exhibits slightly lower emissivity at a given transparency. Emissivity values as low as 0.21 at 78 % visible transparency were achieved. It should be noted that for various applications such as architectural glass or energy-saving windows, where high transparency is a crucial factor, an emissivity value below 0.4 is already perfectly suitable.[33] Recently, low emissivity coatings have also been studied in hybrid photovoltaic-thermal devices. Enhanced performances of such devices were observed with incorporated layers having emissivity values in the range 0.13 – 0.25.[34,35] This means that a large range of applications could be targeted with a fine control of the AgNW dimensions and loadings.

Although these results are very promising, from an applicative point of view, a sole deposition of AgNWs on surfaces does not appear realistic. Indeed, AgNWs adhesion on surfaces such as glass or plastic is not strong. Such unprotected layers are very prone to degradation due to rubbing or scratching processes.[29] In addition, environmental conditions can also lead to silver oxidation or sufidation.[36,37] It thus seems necessary for both product life-time and nanosafety issues[27,38–40] to ensure long-term preservation of the coating performances. To this end, an efficient encapsulating system is searched for.

The choice of possible protective coatings should be carefully considered since they can strongly alter the intrinsic performances of the active layer.[41] The improvement of the adhesive and mechanical properties should not come at the expense of the optical properties. Three different

approaches were considered in this work. The first one is a solution-based technique that consists in the deposition of a thin layer of material by dipping the substrate in a solution. Two different coatings were applied by this method. First an antireflective silica coating based on the polymerization of tetraethoxysilane (TEOS) through sol-gel processing in the presence of ammonia, a basic modifier, was evaluated.[42] Second, a commercial polysiloxane varnish (AE12) was assessed onto the AgNW networks. Just after being dip-coated under optimized conditions, the rear face of the substrates was rinsed with ethanol. The samples were then cured at 100 °C for 1 h to ensure full reticulation of the polymer.

The second coating method relied on vacuum based deposition techniques of three materials, namely indium tin zinc oxide (ITZO), aluminum doped zinc oxide (AZO) and silicon oxycarbide (SiOC). ITZO and 4% Al doped AZO were deposited by physical vapor deposition (PVD) whereas SiOC was prepared by plasma enhanced chemical vapor deposition (PECVD) from octamethylcyclotetrasiloxane.

The third family of coatings was prepared by spatial atomic layer deposition (SALD), a recent open-air, high-throughput technique that has proven to be an effective approach to deposit protective coatings for metallic nanowire networks.[26,43,44] AZO, ZnO and alumina (Al_2O_3) were evaluated and benchmarked with the other techniques. Optical measurements in terms of transmittance and emissivity variations were performed on all samples and compared to bare AgNW networks. The results are presented in Figure 3.

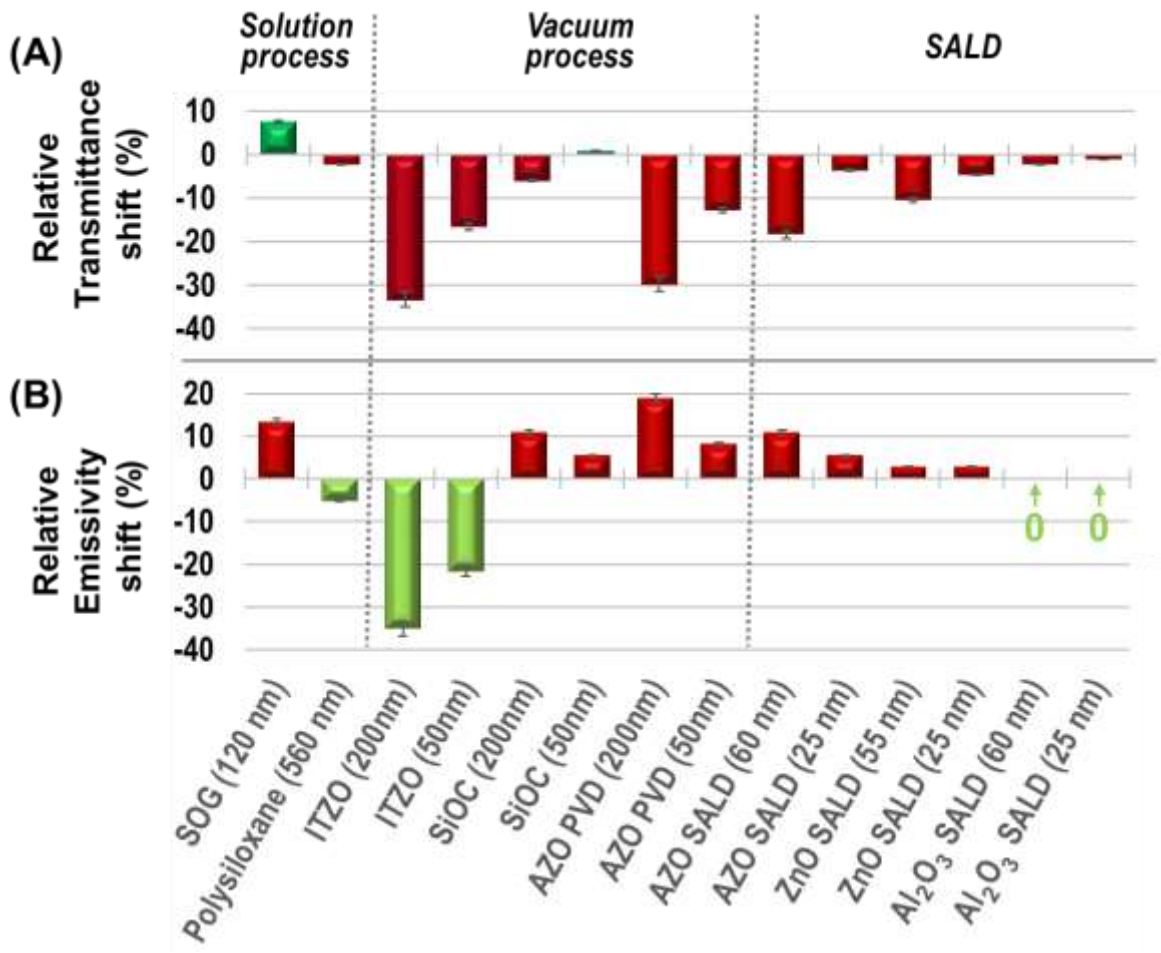

Figure 3. Protective layer impact on low-E coating optical properties: (a) Relative transmittance (measured at 550 nm) shift and (b) relative emissivity shift (2-20 µm) induced by deposition of different protective layers on AgNWs networks, when compared to the non-coated AgNW network.

As shown in Figure 3a, the transmittance of the networks was altered for all the coatings. Positive variation of the transmittance were noted for SiOC and SOG, which was expected regarding their known antireflective properties.[42,45,46] This means that the transmittance was slightly enhanced, in particular by the SOG layer. For all other coatings, decreases in transmittance were measured, with significant discrepancy. ITZO lowered drastically the transmittance as well as PVD deposited AZO. The smallest losses of transmittance (< 5%) were observed for the polysiloxane varnish and

thin alumina layers made by SALD. Regarding the emissivity (Figure 3b), ITZO led to a high decrease whereas most of the other materials induced a positive shift. The most interesting combination thus appears to be a thin layer of alumina deposited by SALD. For 30 and 60 cycles of SALD deposition, *i.e.* about 25 and 60 nm thick coatings, both the transmittance and the emissivity values remain almost unaffected. This is a very interesting result since it gives access to a very thin protecting layer which does not induce a significant modification of the optical properties.

To be of tangible interest, the coating should combine a set of properties in addition to maintaining the intrinsic optical properties of these low-E coatings. Among the expected assets of the encapsulating layer, resilience to peeling and scratching is crucial. We performed specific experiments to tackle this issue. First a simple peeling test was carried out with a Crystal Scotch® from 3M™ to assess the potential change in adhesion after the coating deposition. The second test we performed was based on the ISO 2409 Standard method, a protocol for assessing the resistance of the coatings to separation from substrates when a right-angle lattice pattern is cut into the coating, penetrating through to the substrate. The main results obtained from optical and mechanical characterizations are summarized in Table 1. As shown previously, a thin oxide coating on AgNW or CuNW clearly improve network's stability compared to bare AgNWs[29,30,43,44]. While this long term stability was not investigated in depth in the present article, we observed that the emissivity values of the coated AgNW network have not changed over a period longer than 12 months ago, which is indicative of their stability.

Table 1. Compilation of the optical and mechanical results of the encapsulated AgNWs based low-E coatings, for which several methods and protective coatings were investigated. Colored spots are indicative of the degradation evaluation after the peeling test (green = not visible, orange = slight, red = strong) and the scratch test (green = not visible, orange < 5% of the tested surface and red > 5% of the tested surface). Colors are also used for changes in transmittance (T) and emissivity (E): Green T<3% and E<1%, Orange 3%<T<10% and 1%<E<5%, Red 10%<T and 5%<E.

	No protective layer	Liquid process		Vacuum process			SALD		
	-	SOG (120 nm)	Poly siloxane (560 nm)	ITZO (200 nm)	SiOC (200 nm)	AZO (200 nm)	AZO (25 nm)	ZnO (25 nm)	Al_2O_3 (25 nm)
Peeling test	✗	✗	✓	✓	✓	●	●	●	✓
Scratch test	✗	✗	✓	✓	✓	●	✗	●	✓
Transmittance (% at 550 nm)	75.3	80.8	73.5	50.0	70.5	52.6	72.3	71.5	74.1
Emissivity (2-20 µm)	0.39	0.43	0.37	0.24	0.41	0.44	0.39	0.38	0.37

Concerning the mechanical resistance tests, several encapsulating layers appear suitable, for every kind of deposition process. The most valuable coatings, combining optimal marks related to all the parameters included as entries in Table 1, appear to be the polysiloxane varnish and the alumina deposited by SALD. It is worth noting that in addition to the above mentioned performances, both coatings do not alter significantly the haze factor, the variation being limited to less than 1 %. More precisely, the best candidate is the process based on the thin Al_2O_3 coating obtained by SALD. In this case, there is almost no change in both transmittance and emissivity, and the

mechanical performances are excellent. One way to further optimize the coating of AgNW network is to consider optical simulations on the system substrate-AgNW network-thin oxide coating as those performed by Aghazadehchors et al..[43] This constitutes one of the prospects of this work in order to efficiently integrate such efficient low-E coating in industrial devices. Finally the polysiloxane coating is also very efficient and very easy to process on large surfaces in ambient conditions.

4. CONCLUSIONS

In this work, AgNW networks have been deposited and carefully investigated for low emissivity applications. A simple physical model is proposed to explain the physical origin of the emissivity dependence with transmittance. A good agreement is obtained in spite of the simplicity of the model. In order to provide mechanically resistant and optically neutral coating for AgNW based low-emissivity layers several deposition methods, as well as different materials, have been investigated. This study demonstrates that the association of spray deposited AgNW networks with different encapsulating layers results in very efficient systems. In particular, SALD deposited thin (25nm) alumina layers proved very effective, and a commercial polysiloxane varnish deposited by simple dip-coating also led to very good results. It is worth mentioning that both techniques are associated with large surface and low-temperature covering feasibility, without the need of expensive vacuum equipment. We hope that the reported approach could expand the use of AgNW based low-E coatings and be implemented for the fabrication of functional products.

ASSOCIATED CONTENT

Supporting Information

Description of the proposed theoretical model (see graphical representation in Figure 2A).

AUTHOR INFORMATION

Corresponding Author

*E-mail: jean-pierre.simonato@cea.fr; caroline.celle@cea.fr

Author Contributions

The manuscript was written through contributions of all authors. All authors have given approval to the final version of the manuscript.

Notes

The authors declare no competing financial interest.

ACKNOWLEDGMENT

The authors thanks Fabrice Emieux for the realization of vacuum processes based depositions. DMR acknowledges funding from the ANR through the project DESPATCH (ANR-16-CE05-0021)

REFERENCES

(1) Wassei, J. K.; Kaner, R. B. Graphene, a Promising Transparent Conductor. *Mater. Today* **2010**, *13* (3), 52–59. https://doi.org/10.1016/S1369-7021(10)70034-1.
(2) Spadafora, E. J.; Saint-Aubin, K.; Celle, C.; Demadrille, R.; Grévin, B.; Simonato, J.-P. Work Function Tuning for Flexible Transparent Electrodes Based on Functionalized Metallic Single Walled Carbon Nanotubes. *Carbon* **2012**, *50* (10), 3459–3464. https://doi.org/10.1016/j.carbon.2012.03.010.
(3) Lee, H. B.; Jin, W.-Y.; Ovhal, M. M.; Kumar, N.; Kang, J.-W. Flexible Transparent Conducting Electrodes Based on Metal Meshes for Organic Optoelectronic Device Applications: A Review. *J. Mater. Chem. C* **2019**, *7* (5), 1087–1110. https://doi.org/10.1039/C8TC04423F.
(4) Gueye, M. N.; Carella, A.; Faure-Vincent, J.; Demadrille, R.; Simonato, J.-P. Progress in Understanding Structure and Transport Properties of PEDOT-Based Materials: A Critical Review. *Prog. Mater. Sci.* **2020**, *108*, 100616. https://doi.org/10.1016/j.pmatsci.2019.100616.
(5) Heydari Gharahcheshmeh, M.; Gleason, K. K. Texture and Nanostructural Engineering of Conjugated Conducting and Semiconducting Polymers. *Mater. Today Adv.* **2020**, *8*, 100086. https://doi.org/10.1016/j.mtadv.2020.100086.
(6) Schultheiss, A.; Carella, A.; Pouget, S.; Faure-Vincent, J.; Demadrille, R.; Revaux, A.; Simonato, J.-P. Water Content Control during Solution-Based Polymerization: A Key to Reach Extremely High Conductivity in PEDOT Thin Films. *J. Mater. Chem. C* **2020**. https://doi.org/10.1039/D0TC04899B.
(7) Ye, S.; Rathmell, A. R.; Chen, Z.; Stewart, I. E.; Wiley, B. J. Metal Nanowire Networks: The Next Generation of Transparent Conductors. *Adv. Mater.* **2014**, *26* (39), 6670–6687. https://doi.org/10.1002/adma.201402710.
(8) Sannicolo, T.; Lagrange, M.; Cabos, A.; Celle, C.; Simonato, J.-P.; Bellet, D. Metallic Nanowire-Based Transparent Electrodes for Next Generation Flexible Devices: A Review. *Small* **2016**, *12* (44), 6052–6075.
(9) Langley, D.; Giusti, G.; Mayousse, C.; Celle, C.; Bellet, D.; Simonato, J.-P. Flexible Transparent Conductive Materials Based on Silver Nanowire Networks: A Review. *Nanotechnology* **2013**, *24* (45), 452001. https://doi.org/10.1088/0957-4484/24/45/452001.
(10) Ding, G.; Clavero, C. Silver-Based Low-Emissivity Coating Technology for Energy-Saving Window Applications. In *Modern Technologies for Creating the Thin-film Systems and Coatings*; Nikitenkov, N. N., Ed.; InTech, 2017. https://doi.org/10.5772/67085.
(11) Wang, J.; Jiu, J.; Nogi, M.; Sugahara, T.; Nagao, S.; Koga, H.; He, P.; Suganuma, K. A Highly Sensitive and Flexible Pressure Sensor with Electrodes and Elastomeric Interlayer Containing Silver Nanowires. *Nanoscale* **2015**, *7* (7), 2926–2932. https://doi.org/10.1039/C4NR06494A.
(12) Mayousse, C.; Celle, C.; Carella, A.; Simonato, J.-P. Synthesis and Purification of Long Copper Nanowires. Application to High Performance Flexible Transparent Electrodes with and without PEDOT:PSS. *Nano Res.* **2014**, *7* (3), 315–324. https://doi.org/10.1007/s12274-013-0397-4.
(13) Jones, R.; Draheim, R.; Roldo, M. Silver Nanowires: Synthesis, Antibacterial Activity and Biomedical Applications. *Appl. Sci.* **2018**, *8* (5), 673. https://doi.org/10.3390/app8050673.
(14) Papanastasiou, D. T.; Schultheiss, A.; Muñoz-Rojas, D.; Celle, C.; Carella, A.; Simonato, J.-P.; Bellet, D. Transparent Heaters: A Review. *Adv. Funct. Mater.* **2020**, 1910225. https://doi.org/10.1002/adfm.201910225.

(15) Celle, C.; Mayousse, C.; Moreau, E.; Basti, H.; Carella, A.; Simonato, J.-P. Highly Flexible Transparent Film Heaters Based on Random Networks of Silver Nanowires. *Nano Res.* **2012**, *5* (6), 427–433. https://doi.org/10.1007/s12274-012-0225-2.
(16) Zhao, Q.; Zhao, M.; Qiu, J.; Lai, W.-Y.; Pang, H.; Huang, W. One Dimensional Silver-Based Nanomaterials: Preparations and Electrochemical Applications. *Small* **2017**, *13* (38), 1701091. https://doi.org/10.1002/smll.201701091.
(17) Jung, J.; Cho, H.; Yuksel, R.; Kim, D.; Lee, H.; Kwon, J.; Lee, P.; Yeo, J.; Hong, S.; Unalan, H. E.; Han, S.; Ko, S. H. Stretchable/Flexible Silver Nanowire Electrodes for Energy Device Applications. *Nanoscale* **2019**, *11* (43), 20356–20378. https://doi.org/10.1039/C9NR04193A.
(18) Jelle, B. P.; Kalnæs, S. E.; Gao, T. Low-Emissivity Materials for Building Applications: A State-of-the-Art Review and Future Research Perspectives. *Energy Build.* **2015**, *96*, 329–356. https://doi.org/10.1016/j.enbuild.2015.03.024.
(19) Lim, T.; Jeong, S.-M.; Seo, K.; Pak, J. H.; Choi, Y. K.; Ju, S. Development of Fiber-Based Active Thermal Infrared Camouflage Textile. *Appl. Mater. Today* **2020**, *20*, 100624. https://doi.org/10.1016/j.apmt.2020.100624.
(20) Hsu, P.-C.; Liu, X.; Liu, C.; Xie, X.; Lee, H. R.; Welch, A. J.; Zhao, T.; Cui, Y. Personal Thermal Management by Metallic Nanowire-Coated Textile. *Nano Lett.* **2015**, *15* (1), 365–371. https://doi.org/10.1021/nl5036572.
(21) Larciprete, M. C.; Albertoni, A.; Belardini, A.; Leahu, G.; Li Voti, R.; Mura, F.; Sibilia, C.; Nefedov, I.; Anoshkin, I. V.; Kauppinen, E. I.; Nasibulin, A. G. Infrared Properties of Randomly Oriented Silver Nanowires. *J. Appl. Phys.* **2012**, *112* (8), 083503. https://doi.org/10.1063/1.4759374.
(22) Bobinger, M.; Angeli, D.; Colasanti, S.; La Torraca, P.; Larcher, L.; Lugli, P. Infrared, Transient Thermal, and Electrical Properties of Silver Nanowire Thin Films for Transparent Heaters and Energy-Efficient Coatings: IR, Transient Thermal, and Electrical Properties of Silver NW Thin Films. *Phys. Status Solidi A* **2017**, *214* (1), 1600466. https://doi.org/10.1002/pssa.201600466.
(23) Atkinson, J.; Goldthorpe, I. A. Near-Infrared Properties of Silver Nanowire Networks. *Nanotechnology* **2020**, *31* (36), 365201. https://doi.org/10.1088/1361-6528/ab94de.
(24) Pantoja, E.; Bhatt, R.; Liu, A.; Gupta, M. C. Low Thermal Emissivity Surfaces Using AgNW Thin Films. *Nanotechnology* **2017**, *28* (50), 505708. https://doi.org/10.1088/1361-6528/aa96c2.
(25) Lin, S.; Wang, H.; Zhang, X.; Wang, D.; Zu, D.; Song, J.; Liu, Z.; Huang, Y.; Huang, K.; Tao, N.; Li, Z.; Bai, X.; Li, B.; Lei, M.; Yu, Z.; Wu, H. Direct Spray-Coating of Highly Robust and Transparent Ag Nanowires for Energy Saving Windows. *Nano Energy* **2019**, *62*, 111–116. https://doi.org/10.1016/j.nanoen.2019.04.071.
(26) Muñoz-Rojas, D.; Maindron, T.; Esteve, A.; Piallat, F.; Kools, J. C. S.; Decams, J.-M. Speeding up the Unique Assets of Atomic Layer Deposition. *Mater. Today Chem.* **2019**, *12*, 96–120. https://doi.org/10.1016/j.mtchem.2018.11.013.
(27) Toybou, D.; Celle, C.; Aude-Garcia, C.; Rabilloud, T.; Simonato, J.-P. A Toxicology-Informed, Safer by Design Approach for the Fabrication of Transparent Electrodes Based on Silver Nanowires. *Environ. Sci. Nano* **2019**, *6* (2), 684–694. https://doi.org/10.1039/C8EN00890F.
(28) Mayousse, C.; Celle, C.; Moreau, E.; Mainguet, J.-F.; Carella, A.; Simonato, J.-P. Improvements in Purification of Silver Nanowires by Decantation and Fabrication of

Flexible Transparent Electrodes. Application to Capacitive Touch Sensors. *Nanotechnology* **2013**, *24* (21), 215501. https://doi.org/10.1088/0957-4484/24/21/215501.
(29) Khan, A.; Nguyen, V. H.; Muñoz-Rojas, D.; Aghazadehchors, S.; Jiménez, C.; Nguyen, N. D.; Bellet, D. Stability Enhancement of Silver Nanowire Networks with Conformal ZnO Coatings Deposited by Atmospheric Pressure Spatial Atomic Layer Deposition. *ACS Appl. Mater. Interfaces* **2018**, *10* (22), 19208–19217. https://doi.org/10.1021/acsami.8b03079.
(30) Nguyen, V. H.; Resende, J.; Papanastasiou, D. T.; Fontanals, N.; Jiménez, C.; Muñoz-Rojas, D.; Bellet, D. Low-Cost Fabrication of Flexible Transparent Electrodes Based on Al Doped ZnO and Silver Nanowire Nanocomposites: Impact of the Network Density. *Nanoscale* **2019**, *11* (25), 12097–12107. https://doi.org/10.1039/C9NR02664A.
(31) Celle, C.; Mayousse, C.; Moreau, E.; Basti, H.; Carella, A.; Simonato, J.-P. Highly Flexible Transparent Film Heaters Based on Random Networks of Silver Nanowires. *Nano Res.* **2012**, *5* (6), 427–433. https://doi.org/10.1007/s12274-012-0225-2.
(32) Lagrange, M.; Langley, D. P.; Giusti, G.; Jiménez, C.; Bréchet, Y.; Bellet, D. Optimization of Silver Nanowire-Based Transparent Electrodes: Effects of Density, Size and Thermal Annealing. *Nanoscale* **2015**, *7* (41), 17410–17423. https://doi.org/10.1039/C5NR04084A.
(33) Giovannetti, F.; Föste, S.; Ehrmann, N.; Rockendorf, G. High Transmittance, Low Emissivity Glass Covers for Flat Plate Collectors: Applications and Performance. *Sol. Energy* **2014**, *104*, 52–59. https://doi.org/10.1016/j.solener.2013.10.006.
(34) Lämmle, M.; Kroyer, T.; Fortuin, S.; Wiese, M.; Hermann, M. Development and Modelling of Highly-Efficient PVT Collectors with Low-Emissivity Coatings. *Sol. Energy* **2016**, *130*, 161–173. https://doi.org/10.1016/j.solener.2016.02.007.
(35) Alonso-Álvarez, D.; Ferre Llin, L.; Mellor, A.; Paul, D. J.; Ekins-Daukes, N. J. ITO and AZO Films for Low Emissivity Coatings in Hybrid Photovoltaic-Thermal Applications. *Sol. Energy* **2017**, *155*, 82–92. https://doi.org/10.1016/j.solener.2017.06.033.
(36) Deignan, G.; Goldthorpe, I. A. The Dependence of Silver Nanowire Stability on Network Composition and Processing Parameters. *RSC Adv* **2017**, *7* (57), 35590–35597. https://doi.org/10.1039/C7RA06524H.
(37) Mayousse, C.; Celle, C.; Fraczkiewicz, A.; Simonato, J.-P. Stability of Silver Nanowire Based Electrodes under Environmental and Electrical Stresses. *Nanoscale* **2015**, *7* (5), 2107–2115. https://doi.org/10.1039/C4NR06783E.
(38) Lehmann, S. G.; Toybou, D.; Pradas del Real, A.-E.; Arndt, D.; Tagmount, A.; Viau, M.; Safi, M.; Pacureanu, A.; Cloetens, P.; Bohic, S.; Salomé, M.; Castillo-Michel, H.; Omaña-Sanz, B.; Hofmann, A.; Vulpe, C.; Simonato, J.-P.; Celle, C.; Charlet, L.; Gilbert, B. Crumpling of Silver Nanowires by Endolysosomes Strongly Reduces Toxicity. *Proc. Natl. Acad. Sci.* **2019**, *116* (30), 14893–14898. https://doi.org/10.1073/pnas.1820041116.
(39) Cui, R.; Chae, Y.; An, Y.-J. Dimension-Dependent Toxicity of Silver Nanomaterials on the Cladocerans Daphnia Magna and Daphnia Galeata. *Chemosphere* **2017**, *185*, 205–212. https://doi.org/10.1016/j.chemosphere.2017.07.011.
(40) Charehsaz, M.; Coskun, S.; Unalan, H. E.; Reis, R.; Helvacioglu, S.; Giri, A. K.; Aydin, A. Genotoxicity Study of High Aspect Ratio Silver Nanowires. *Toxicol. Environ. Chem.* **2017**, *99* (5–6), 837–847. https://doi.org/10.1080/02772248.2016.1276581.
(41) Bang, J.; Coskun, S.; Pyun, K. R.; Doganay, D.; Tunca, S.; Koylan, S.; Kim, D.; Unalan, H. E.; Ko, S. H. Advances in Protective Layer-Coating on Metal Nanowires with

Enhanced Stability and Their Applications. *Appl. Mater. Today* **2021**, *22*, 100909. https://doi.org/10.1016/j.apmt.2020.100909.
(42) Pénard, A.-L.; Gacoin, T.; Boilot, J.-P. Functionalized Sol–Gel Coatings for Optical Applications. *Acc. Chem. Res.* **2007**, *40* (9), 895–902. https://doi.org/10.1021/ar600025j.
(43) Aghazadehchors, S.; Nguyen, V. H.; Muñoz-Rojas, D.; Jiménez, C.; Rapenne, L.; Nguyen, N. D.; Bellet, D. Versatility of Bilayer Metal Oxide Coatings on Silver Nanowire Networks for Enhanced Stability with Minimal Transparency Loss. *Nanoscale* **2019**, *11* (42), 19969–19979. https://doi.org/10.1039/C9NR05658K.
(44) Celle, C.; Cabos, A.; Fontecave, T.; Laguitton, B.; Benayad, A.; Guettaz, L.; Pélissier, N.; Nguyen, V. H.; Bellet, D.; Muñoz-Rojas, D.; Simonato, J.-P. Oxidation of Copper Nanowire Based Transparent Electrodes in Ambient Conditions and Their Stabilization by Encapsulation: Application to Transparent Film Heaters. *Nanotechnology* **2018**, *29* (8), 085701. https://doi.org/10.1088/1361-6528/aaa48e.
(45) Bautista, M. C.; Morales, A. Silica Antireflective Films on Glass Produced by the Sol–Gel Method. *Sol. Energy Mater. Sol. Cells* **2003**, *80* (2), 217–225. https://doi.org/10.1016/j.solmat.2003.06.004.
(46) Babich, K.; Fukiage, N.; Mahorowala, A.; Halle, S.; Bunner, T.; Pfeiffer, D.; Mochiki, H.; Ashigaki, S.; Xia, A.; Angelopoulos, M. A Novel Graded Antireflective Coating with Built-in Hardmask Properties Enabling 65nm and below CMOS Device Patterning. In *IEEE International Electron Devices Meeting 2003*; IEEE: Washington, DC, USA, 2003; p 28.5.1-28.5.4. https://doi.org/10.1109/IEDM.2003.1269369.